Thermodynamic Stability of the Two Isoforms of Bovine Seminal Ribonuclease†

Concetta Giancola,‡ Pompea Del Vecchio,‡ Claudia De Lorenzo,§ Roberto Barone,§ Renata Piccoli,§ Giuseppe D'Alessio,*,§ and Guido Barone*,‡

Department of Chemistry, University "Federico II" of Naples, Via Mezzocannone 4, 80134 Naples, Italy, Department of Organic and Biological Chemistry, University "Federico II" of Naples, Via Mezzocannone 16, 80134 Naples, Italy

Received December 27, 1999; Revised Manuscript Received May 1, 2000

ABSTRACT: Bovine seminal ribonuclease (BS-RNase) is a dimeric protein with two identical subunits linked by two disulfide bridges, each subunit showing 80% of sequence identity with pancreatic RNase A. BS-RNase exists in two different quaternary conformations in solution: the M×M form, in which each subunit exchanges its α-helical N-terminal segment with its partner, and the M═M form with no exchange. By differential scanning microcalorimetry (DSC), the denaturation of the two dimeric forms of BS-RNase was found to be more complex than a simple two-state process. Monomeric derivatives of the dimeric protein follow instead a simple two-state mechanism, but are distinctly less stable than RNase A. The three-state N ⇔ I ⇔ D denaturation process of the two quaternary isoforms was interpreted by identifying in the dimers a central highly structured core, enclosing the covalently bonded subunit interface, which unfolds only after the periphery (mainly the N-terminal peptide) unfolds. Circular dichroism spectra of the two forms in the far-ultraviolet region show large differences between the secondary structure of the isoforms and that of the native BS-RNase mixture at equilibrium. This has been attributed to the presence in the equilibrium mixture of intermediate forms with displaced and disordered N-terminal α-helical segments.

Bovine seminal ribonuclease (BS-RNase,[1] see ref *1* for a review) is the only dimeric member of the tetrapod RNase superfamily (*2*), whose monomeric prototype is pancreatic RNase A. BS-RNase is extraordinarily abundant (1.5 mg/mL plasma) in bull semen and has not been found in other, even closely related species. It is an allosteric enzyme in the rate-determining step of the biocatalytic reaction and displays other special biological actions: aspermatogenic and immunosuppressive, and a selective toxicity toward tumor cells, activated T cells, and the male germ cell line.

From a structural point of view, BS-RNase is a dimeric protein formed by two identical subunits linked through two intersubunit disulfide bridges. Each subunit reveals 23 amino acid substitutions when compared with bovine pancreatic RNase A, including two cysteine residues at the positions 31 and 32. These form two intersubunit disulfide bridges with the cysteine residues 32′ and 31′, respectively, of the other subunit. The 8 intrasubunit residues of cysteine, at the same positions and paired as in RNase A, contribute to the compactness of the overall structure. Other important roles are played by the leucine residues at position 28 of each subunit, for the hydrophobic interactions at the intersubunit interface, and by the proline residues at position 19, for the swapping of the N-terminal peptide between subunits (*3*, *4*).

BS-RNase exists in two different quaternary forms: in the first, named M×M, the N-terminal peptide (residues 1−15, mainly in α-helix conformation) is interchanged between subunits (*3*), and in the other, named M═M, the interchange does not occur (*5*) (Figure 1). The two dimeric forms are separable, and stable at 4 °C up to 3 months (*5*). At 37 °C, however, M×M and M═M very slowly transform into each other until at equilibrium, the ratio of M×M to M═M approaches 2:1, the same ratio found in preparations of isolated BS-RNase (*5*). The dimeric structure has been reported to be essential for the antitumor and immunosuppressive activities of the protein (*6*−*8*). Recently, it has been found by different experimental approaches that the M×M form is most active as an antitumor agent, and perhaps it is the only quaternary form with antitumor (*4*, *9*, *10*) and aspermatogenic activity (*10*). Furthermore, the M×M form is responsible for the allosteric properties of native BS-RNase (*5*).

The intersubunit disulfide bridges of BS-RNase can be selectively reduced (*11*) and the sulfhydryl groups stabilized by alkylation with iodoacetic acid or iodoacetamide, to obtain a doubly carboxymethylated (MCM-BS-RNase) (*11*) or carboxyamidomethylated (MCAM-BS-RNase) (*12*) monomer, respectively. These monomers have a higher ribonuclease activity than the parent dimeric enzyme (*13*), but do not possess the special, noncatalytic actions of native BS-RNase (*7*, *8*).

In previous works we have analyzed the thermal denaturation of several wild-type and mutant monomeric ribo-

† This work was supported by grants of the Italian Ministry of University and Scientific and Technological Research (MURST, Rome. Programs COFIN.MURST of national interest).

* To whom correspondence should be addressed. E-mail: barone@chemna.dichi.unina.it. Phone: (+039) 081-5476502/508. Fax: (+039) 081-5527771.

‡ Department of Chemistry.

§ Department of Organic and Biological Chemistry.

[1] Abbreviations: BS-RNase, bovine seminal ribonuclease; M×M, M═M, the quaternary forms of BS-RNase; I×I, I═I, the intermediate conformers generated from the M×M and M═M forms, respectively, in their denaturation processes; CU, number of cooperative units.

10.1021/bi992953j CCC: $19.00
Published on Web 06/14/2000

FIGURE 1: (Top) Structure of the M×M form of BS-RNase redrawn from the originals (refs *1* and *3*) using the MOLSCRIPT program. (Bottom) A model of the quaternary structure of the M═M form of BS-RNase based on the RNase A structure, redrawn from the original (ref *1*).

nucleases (*14*−*17*) and preliminarily analyzed (*18*) the thermal denaturation of native BS-RNase (i.e., the natural mixture of M×M and M═M). In this paper, we have studied by differential scanning calorimetry (DSC) the stability of the isolated M×M and M═M forms, and of a stable monomeric derivative of BS-RNase (MCM-BS-RNase) at pH 3.0, 5.0, and 8.4. The results were compared with those obtained for BS-RNase, the natural mixture of quaternary forms, and RNase A. Circular dichroism (CD) spectra of the dimeric forms and of the monomeric derivative at 25 °C, at the same pH values as for DSC, have also been compared with those of native BS-RNase and RNase A. The results from the DSC analyses, and from the deconvolution of the DSC curves, suggest that BS-RNase isoforms denature with a three-state process, in which the protein peripheral regions unfold first, followed by the unfolding of the central cores of the dimers. Small, but significant differences have been detected in the fine structure of the CD far-ultraviolet spectra of the isoforms, a fine structure which disappears when upon incubation the equilibrium mixture typical of native BS-RNase is established.

EXPERIMENTAL PROCEDURES

Materials. A modification (*19*) of a previously described procedure (*20*) was used for the purification of BS-RNase. Briefly, the heat step was omitted, and diluted seminal plasma was directly applied onto a carboxymethyl-cellulose column equilibrated at pH 8.0 with 0.1 M Tris-HCl containing 0.1 M NaCl. After extensive washing with the same buffer until the abosrbancy at 280 nm was lower than 0.1, BS-RNase was eluted by increasing the concentration of NaCl to 0.3 M. The M×M and M═M forms of seminal RNase were obtained from BS-RNase by selective reduction of the two intersubunit disulfide bridges, followed by separation by gel filtration of the noncovalent dimer (NCD) and the monomeric (M) species, and by the reoxidation of the intersubunit disulfides of NCD and M, which gives the M×M and M═M forms, respectively (*5*). The carboxymethylated monomer derivative, MCM-BS-RNase, was prepared by selective reduction with dithiothreitol of the two disulfide bridges (at positions 31 and 32) of the native dimeric protein, followed by *S*-alkylation with iodoacetic acid (*11*).

Bovine pancreatic RNase A was a Sigma product (Type XII-A), used without any further treatment. Protein concentration was determined by absorption spectroscopy using the extinction coefficient $A_{278}^{0.1\%} = 0.46$ for the dimeric proteins (21), $A_{278}^{0.1\%} = 0.71$ for RNase A (*22*) and $A_{278}^{0.1\%} = 0.54$ for the monomeric derivatives of BS-RNase (*12*). Buffers, prepared with Sigma products, were 0.1 M glycine-HCl at pH 3.0, 0.1 M sodium acetate at pH 5.0, and 0.1 M Tris-acetate at pH 8.4. The pH of the solutions was determined by a Radiometer pH meter model PHM 93 at 25 °C.

Differential Scanning Calorimetry. DSC analysis was performed on a second generation Setaram Micro-DSC at 0.5 °C min^{-1}. Decreasing or increasing the heating rate to 0.3 or 1 K min^{-1}, respectively, did not change the thermodynamic parameters significantly. The calorimetric unit was interfaced to an IBM PC computer for automatic data collection and analysis using previously described software (*23*). The apparent molar heat capacity curves were obtained by correcting each calorimetric curve for the instrument calibration curve and the buffer-buffer scanning curve, and dividing each data point by the scan rate and the number of protein moles in the sample cell. The performance of the instrument was calibrated periodically with an electrical pulse.

Finally, the apparent molar heat capacities were converted to the excess molar heat capacities $\langle \Delta C_p(T) \rangle$ assuming the native state heat capacities as the reference baseline, according to the procedure of Freire and Biltonen (*24*). The total experimental calorimetric enthalpy, $\Delta_d H$, was determined by integration of the area under the curve. The van't Hoff enthalpy was calculated by the calorimetric data according to Privalov, assuming as a preliminary hypothesis that a two-state N ⇔ D transition occurs (*25*):

$$\Delta_d H_{vH} = 4RT_{max}^2 \langle \Delta_d C_p(T_{max}) \rangle / \Delta_d H \qquad (1)$$

where T_{max} is the maximum of the DSC peak, $\langle \Delta_d C_p(T_{max}) \rangle$ is the value of the excess heat capacity function at T_{max}, and R is the gas constant. The number of cooperative units (CU) was calculated as the calorimetric to van't Hoff enthalpy ratio: $CU = \Delta_d H / \Delta_d H_{vH}$. Only under the necessary condition that CU is unitary it can be correctly assumed that the denaturation is a two-state transition and $T_{max} = T_d$, the midpoint denaturation temperature, otherwise a more complex model must be searched.

Circular Dichroism Spectra. Circular dichroic (CD) spectra were obtained by a Jasco J-710 dichrograph equipped with thermostatic cuvette holder (JASCO PTC-348) that allows measurements at controlled temperature. The spectra were recorded at a scanning rate of 2 nm s^{-1}. The protein solutions were analyzed in 0.1 or 0.5 cm optical path cells in the far-ultraviolet and near-ultraviolet regions, respectively. The reference spectra of the buffer were obtained in the same conditions.

CD results were expressed as mean residue ellipticities (degree cm^2 dmol^{-1}) utilizing 117 as the mean residue molecular weight for M×M, M═M, and monomeric BS-RNase (*26*) and 110.5 for RNase A (*27*). The buffer was 0.01 M Tris-acetate, and the protein concentration was in the 0.2 and 3.0 mg/mL ranges for the measurements in the far- and near-ultraviolet regions, respectively. The reported CD values were averages of at least five independent determinations.

Table 1: Thermodynamic Parameters of the Thermal Denaturation Process of BS-RNase Forms Compared with RNase A at Different pH Values

	T_{max}[a] (°C)	$\Delta_d H$ (kJ mol^{-1})	CU[b]
pH 3.0			
M×M	52.6	590 ± 12	2.1
M═M	50.6	552 ± 18	2.1
MCM-BS-RNase	42.2	302 ± 10	1.0
RNase A	52.4	413 ± 12	0.9
pH 5.0			
M×M	61.4	643 ± 20	2.1
M═M	61.3	612 ± 17	2.0
BS-RNase[c]	61.6	633 ± 10	1.7
MCM-BS-RNase	55.8	370 ± 9	1.0
RNase A	61.3	465 ± 10	1.1
pH 8.4			
M×M[d]	64.9	858 ± 25	
M═M[d]	64.6	798 ± 21	
BS-RNase[c,d]	65.2	833 ± 17	
MCM-BS-RNase	57.8	382 ± 11	1.0
RNase A[d]	64.1	523 ± 12	

[a] The error in T_{max} does not exceed 0.2 °C. [b] Number of cooperative units $CU = \Delta_d H / \Delta_d H_{vH}$. [c] From ref *18*. [d] Undergoes irreversible denaturation process.

RESULTS AND DISCUSSION

Thermal Denaturation of the Dimeric Forms of BS-RNase. Previously reported preliminary results on native BS-RNase (a 2:1 equilibrium mixture of M×M and M═M forms) suggested that its denaturation cannot be represented by a simple N ⇔ D two-state transition (*18*). The accurate and complex procedure for the isolation of the two quaternary isoforms (*5*) allows now to perform separate denaturation measurements on each isolated form.

The DSC results on the isomeric forms at pH 3.0, 5.0, and 8.4 are collected in Table 1, as averaged values of at least three measurements. The calorimetric profiles of M×M and M═M at different pH values are shown in Figure 2. The thermal denaturations at pH 3.0 and 5.0 are reversible processes for both dimeric forms, i.e., a second heating of the protein solution, previously cooled to room temperature, gave a calorimetric curve largely superimposable to that obtained with the first heating. In addition, calorimetric experiments in the isothermal mode have been carried out for several hours at temperatures near the incipient denaturation ranges to promote interconversion of the pure forms. However, no thermal effects were detected during the experimental procedures. We have also checked that during the heating procedure no appreciable interconversion occurs. At pH 8.4, the denaturation process is irreversible, probably because the proteins undergo side reactions, favored by temperature and alkalinity, which prevent the refolding of the proteins on cooling. The same occurs for RNase A (*18*).

On increasing the pH, both T_{max} and $\Delta_d H$ values rise. This stabilizing effect finds an explanation in the principles of the electrostatic theory that predict the maximum of stability near the isoelectric point of the protein, where the net charge is zero (*28*). Since the isoelectric point for BS-RNase was found to be 10.3 (*21*), an increase of stability on increasing the pH is expected.

There are small differences between the $\Delta_d H$ and T_{max}

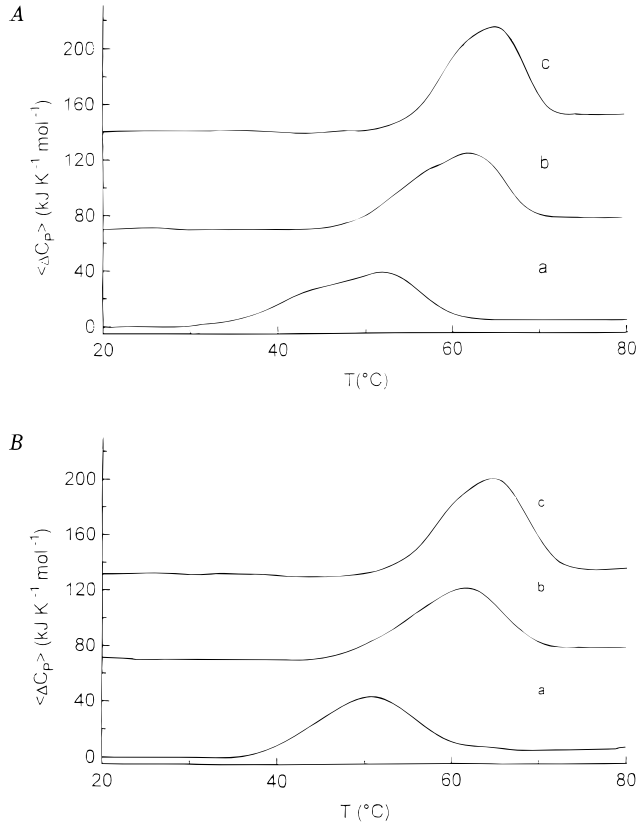

FIGURE 2: Experimental DSC profiles of the M×M form (panel A) and M═M form (panel B) at pH 3.0 (curve a), pH 5.0 (curve b) and pH 8.4 (curve c). The curves b and c are shifted along the *y*-axis for ease of presentation.

values of the two forms, close to the experimental uncertainty. However, the values of $\Delta_d H$ at each pH were consistently found to be a little higher for M×M than for M═M, with the native BS-RNase mixture showing intermediate values. This may be interpreted (see below) as due to the higher degree of structural complexity in the M×M form that arises from the interchange of the N-terminal arms occurring between the subunits (see Figure 1).

The T_{max} values of M×M and M═M, at each pH, are close to the corresponding T_d values found for RNase A, but higher than those found for the monomeric derivative of BS-RNase (see Table 1). The denaturation molar enthalpies for the dimers are lower than twice the $\Delta_d H$ value of pancreatic RNase A, despite their double molecular weight, but roughly twice that of their own monomer. The overall denaturation heat capacity change, $\Delta_d C_P$, being practically pH independent, is simply averaged on the experimental values obtained at the three pH values. The values result to be 10.7 ± 0.2 and 10.3 ± 0.2 kJ K^{-1} mol^{-1} for M×M and M═M, respectively, and are about twice those of the monomeric derivative. The number of cooperative units for both isoforms is greater than unity (Table 1) at pH 3.0 and 5.0. This indicates that the calorimetric curves cannot be represented by a two-state transition model.

The DSC curves were thus analyzed using a deconvolution procedure according to a two-sequential transition model. This model considers the presence of an intermediate state between the native and denatured ones, according to the scheme

$$N \overset{K_1}{\longleftrightarrow} I \overset{K_2}{\longleftrightarrow} D \quad (2)$$

where I is an intermediate state in the sequential passage from native (N) to denatured (D) state. The K_1 and K_2 values are temperature-dependent according to

$$K_1 = \exp - \{[\Delta_N^I H(T_{d1})/R(1/T - 1/T_{d1})] + (\Delta_N^I C_p/R)\,[1 - (T_{d1}/T) - \ln(T/T_{d1})]\} \quad (3)$$

and

$$K_2 = \exp - \{[\Delta_I^D H(T_{d2})/R\,(1/T - 1/T_{d2})] + (\Delta_I^D C_p/R)\,[1 - (T_{d2}/T) - \ln(T/T_{d2})]\} \quad (4)$$

where T_{d1} and T_{d2} are the denaturation temperatures when K_1 and K_2 are respectively unitary, $\Delta_N^I H(T_{d1})$ and $\Delta_I^D H(T_{d2})$ are the enthalpy changes associated with the N ⇔ I and I ⇔ D conformational transitions, respectively, and $\Delta_N^I C_p(T_{d1})$ and $\Delta_I^D C_p(T_{d2})$ are the corresponding heat capacity changes.

Equations 3 and 4 are exact on the assumption that the heat capacity changes are temperature-independent, otherwise their explicit dependence must be accounted for.

The canonical partition function $Q(T)$ for this process, is given (*24*) by

$$Q(T) = [N] + [I] + [D] \quad (5)$$

Taking the native state as a reference, it becomes

$$Q_N(T) = 1 + K_1 + K_1K_2 \quad (6)$$

where $Q_N(T)$ is related to the excess enthalpy function, referred to the native state, $\langle \Delta H(T) \rangle_N$, by the general statistical mechanical relationship:

$$\langle \Delta H(T) \rangle_N = RT^2[\partial \ln Q_N(T)/\partial T]_P \quad (7)$$

Expressing this derivative in the explicit form, it is obtained

$$\langle \Delta H(T) \rangle_N = [\Delta_N^I H(T_{d1}) + \Delta_N^I C_p(T - T_{d1})][K_1/Q_N(T)] + [\Delta_N^I H(T_{d1}) + \Delta_N^I C_p(T - T_{d1}) + \Delta_I^D H(T_{d2}) + \Delta_I^D C_p(T - T_{d2})][K_1K_2/Q_N(T)] \quad (8)$$

The excess heat capacity function, the physical observable of the DSC measurements, is finally given by

$$\langle \Delta C_p(T) \rangle = [\partial \langle \Delta H(T) \rangle_N/\partial T]_P \quad (9)$$

The DSC curves are simulated using as input parameters the values of T_{d1}, $\Delta_N^I H(T_{d1})$, $\Delta_N^I C_p$, T_{d2}, $\Delta_I^D H(T_{d2})$, and $\Delta_I^D C_p$. To reduce the number of independent parameters, the total heat capacity change associated with the overall transition, $\Delta_d C_p = \Delta_N^I C_p + \Delta_I^D C_p$, was subtracted using an iterative procedure (*29*, *30*). In this manner, the number of parameters to simulate a DSC curve becomes 4. We used a program that allows the deconvolution of an experimental curve with respect to eq 9, using the Levenberg−Marquardt algorithm (*31*) as implemented in the Optimization Toolbox of MATLAB. This program was already applied successfully to yeast hexokinase (*32*).

Table 2: Thermodynamic Parameters of the Deconvolution Analysis of M×M and M═M dimers at pH 3.0 and 5.0

	pH	T_{d1} (°C)	$\Delta_{d1}H$ (kJ mol^{-1})	T_{d2} (°C)	$\Delta_{d2}H$ (kJ mol^{-1})
M×M	3.0	44.4	264	52.9	318
M═M	3.0	46.5	264	52.5	300
M×M	5.0	55.2	300	62.0	368
M═M	5.0	57.0	290	63.4	340

The results of the deconvolution of experimental curves for M×M and M═M at pH 3.0 and 5.0 are collected in Table 2. The deconvolution procedure was not applied at pH 8.4, as the denaturation process was found to be irreversible. The calculated profiles superimposed to the experimental curves are shown in the Figures 3. The agreement between the calculated and experimental profiles is satisfactory. Other interpretative models (a two-independent transition model or a three-step sequential model) gave a worse agreement with the experimental results.

An interpretation of these data can be based on the following considerations: (i) the central part of the macromolecule is stabilized by the interchain disulfide bridges and by hydrophobic interactions involving Leu and Met residues protruding in the interface between the subunits; (ii) the two subunits are identical in each isoform and related by pseudo-symmetry axis (*3*); (iii) it has been found that, in contrast with the free protein in solution, a constrained RNase A (structurally homologous to a BS-RNase subunit) when immobilized on a polymeric matrix shows a more complex denaturation than a two-state transition (*33*). Thus, a subunit of BS-RNase can be considered as a RNase moiety constrained by covalent links (the two intersubunit disulfides) to an identical RNase moiety. Hence, the first transition N ⇔ I in the unfolding of M×M or M═M, defined by lower enthalpy and T_d values, may be attributed to the denaturation of peripheral zones of the macromolecule, including the two N-terminal peptides.

This interpretation is supported by previous findings obtained in the analysis of the denaturation of RNase S, the stoichiometric complex of the S-protein (the RNase A core) with 21-residue N-terminal S-peptide (*16*). Interestingly, the enthalpy calculated for the first step of M×M or M═M denaturation is comparable to about twice that evaluated for the dissociation-unfolding process, in substoichiometric conditions, of the S-peptide (mainly in α-helix conformation in the complex) from RNase S, although in this case there is a complete dissociation of the peptide segment (*34*). In the second transition step, I ⇔ D for both M×M and M═M, the unfolding of the dimeric hydrophobic core occurs, which includes the subunit interface. The denaturation enthalpy values of the central core of each dimeric form, $\Delta_{d2}H$, result greater than the respective $\Delta_{d1}H$. Furthermore, the hypothesis is supported by the results of the CD thermal curves in the far UV (data not shown). These data confirm that for both M×M and M═M isomers the loss of the α-helix content starts at the same temperature value of the thermal denaturation processes detected by DSC measurements and extends through the full range of denaturation.

These considerations are in line with previous findings obtained by probing with trypsin the M×M and M═M isoforms of BS-RNase. The effects of tryptic degradation are different for the isolated M×M and M═M forms, as a different final digestion product is generated for each BS-RNase form, but both products essentially consist of the central part of each parent dimer, with the interfacial zone resistant to trypsin and perfectly preserved (*35*). More recent results in this research line (*36*) have shown that a necessary intermediate(s) in the interconversion process is a subunit with an unfolded N-terminal α-helix. Thus, the early events in the unfolding occur at the periphery of the molecule.

In conclusion, the interpretation proposed above indicates that a comparison between the thermal stability of the isoforms of BS-RNase and that of monomeric analogues is not appropriate, as the structural frameworks of the two dimers under investigation involved in two sequential denaturation transitions, are different from that of each constituent subunit when isolated as a free monomer. This model is substantially different from that discussed by Brandts, Hu, and Lin (*37*), which refers properly to the denaturation of oligomeric proteins with subunits not covalently bonded. In these cases, the first step of the unfolding process is just the destabilization of the interface with the loss of intersubunit interactions. The cases of RNase S, MCM-BS RNase, and RNase A show clearly that one domain monomeric analogues denature with a one-step mechanism, whereas RNase A covalently linked to a matrix behaves as BS-RNase.

The DSC profiles for M×M and M═M at pH 3.0 and 5.0 (Figure 2) differ for the presence of a pronounced shoulder in the case of the M×M form. This is more evident after the deconvolution procedure (Figure 3). The enthalpy changes estimated at these pH values for the first step of denaturation of both the dimeric proteins have very close values, whereas the denaturation temperature is about 2 °C lower for the M×M form. This may appear as paradoxical, given the higher organization of M×M, in which additional intersubunit interactions are present, for the exchange of the N-terminal α-helices between subunits. Preliminary X-ray crystallographic data (*38*), in fact, indicate the lack of a single stable conformation in either subunit of M═M for the linker peptide connecting each N-terminal α-helix to the subunit main body. Likely, these differences in denaturation temperatures are due to the higher entropic gain afforded by the M×M → I×I transition with respect to that for the M═M → I═I. Moreover, the hypothesis that M×M is characterized by a greater connectivity than M═M is also supported by the CD data recorded in the far-UV at 25 °C, as discussed below.

The second step of denaturation is characterized, vice versa, by prevailing enthalpic terms, even if the T_{d2} value for M×M at pH 5.0 is still 1.4 °C lower than the T_{d2} of M═M. This may only be due to a large enthalpy−entropy compensation effect. Actually, at pH 3.0, the enthalpy change, $\Delta_{d2}H$, of M×M is 6% higher than that of M═M, with the entropic difference being 5% higher. The same occurs at pH 5.0 where the difference in enthalpy is 10% higher for M×M and that in entropy 9% higher. These considerations support the hypothesis proposed above, assumed that the intermediate states for the two isoforms are different, whereas the final denatured state is the same. It is reasonable that during the second step the co-presence of denatured molecules may induce, at equilibrium, the interconversion of the forms. It has been underlined above,

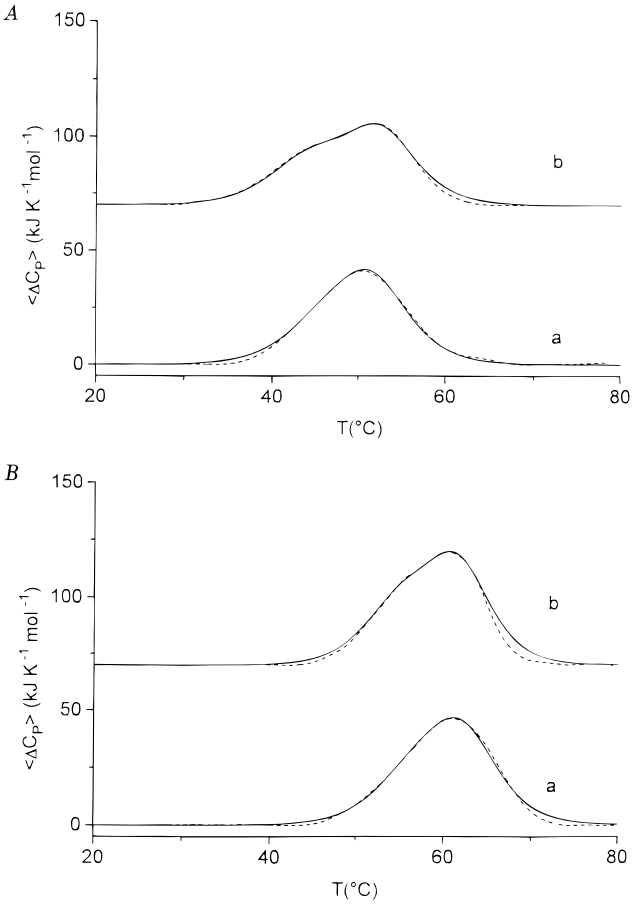

FIGURE 3: (A) Normalized DSC profiles (dashed lines) of M═M form (curve a) and the M×M form (curve b) at pH 5.0. The solid lines represent the best fit according to the thermodynamic model reported in the text. (B) Profiles as panel A at pH 3.0.

Table 3: Comparison between Thermodynamic Parameters of Monomer of BS-RNase and RNase A at the Denaturation Temperature of Monomer, at pH 3.0 and 5.0

pH 3.0	$\Delta_dH(42.2)$ (kJ mol^{-1})	$\Delta_dS(42.2)$ (kJ mol^{-1} K^{-1})	$\Delta_dG(42.2)$ (kJ mol^{-1})
MCM-BS-RNase	302 ± 10	0.96 ± 0.03	0
RNase A	357 ± 12	1.09 ± 0.04	13.3 ± 1.6
pH 5.0	$\Delta_dH(55.8)$ (kJ mol^{-1})	$\Delta_dS(55.8)$ (kJ mol^{-1}K^{-1})	$\Delta_dG(55.8)$ (kJ mol^{-1})
MCM-BS-RNase	370 ± 9	1.12 ± 0.03	0
RNase A	435 ± 10	1.30 ± 0.03	7.4 ± 1.5

however, that the interconversion is practically athermic.

Thermal Denaturation of Monomeric BS-RNase. The calorimetric curves of the carboxy-methylated monomeric derivative (MCM-BS-RNase) show a symmetric shape and the CU value is unitary at all the investigated pHs, so a simple two-state transition model describes the denaturation process, as in the case of RNase A. The experimental thermodynamic data are collected in Table 1.

The denaturation temperature markedly changes from 42.2 °C at pH 3.0 to 55.8 at pH 5.0 and to 57.8 °C at pH 8.4, with Δ_dH values slightly rising upon the increase of pH. The values at pH 5.0 are similar to those reported for the monomeric derivative MCAM-BS-RNase (*39*) (T_d= 55.2 and Δ_dH = 380 ± 12). The Δ_dC_p value was estimated by the slope of the linear plot obtained reporting Δ_dH values as a function of T_d at different pH values, following a procedure first reported by Privalov et al. (*30*). A value of 5.1 ± 0.1 kJ K^{-1} mol^{-1} was obtained, a little lower than the value of 5.5 ± 0.2 kJ K^{-1} mol^{-1} found for RNase A (*17*). According to the currently used model (*40*−*43*), the value obtained for MCM-BS-RNase is due to the exposure to water of apolar residues (not present in the RNase A) originally buried in the native dimeric structure of BS-RNase.

To compare the denaturation enthalpies, entropies, and Gibbs' energies of monomeric BS-RNase and RNase A, we calculated these thermodynamic functions for RNase A at the same denaturation temperatures of MCM-BS-RNase at the respective pH values. Assuming that Δ_dC_p is temperature independent in the narrow range considered here, the denaturation parameters can be calculated according to the well-known thermodynamic relationships:

$$\Delta_dH(T) = \Delta_dH(T_d) + \Delta_dC_p\,(T - T_d) \qquad (11)$$

$$\Delta_dS(T) = [\Delta_dH(T_d)/T_d] + \Delta_dC_p \ln(T/T_d) \qquad (12)$$

$$\Delta_dG(T) = \Delta_dH(T) - T\Delta_dS(T) \qquad (13)$$

The data are collected in Table 3. A comparison of RNase A with the monomeric form of BS-RNase leads to a difference in Gibbs' energy of 13.3 ± 1.6 kJ mol^{-1} at pH 3.0 and 7.4 ± 1.5 kJ mol^{-1} at pH 5.0. The irreversibility of the denaturation process of RNase A at pH 8.4 does not allow for the application of the equations above. The reversibility of the denaturation of BS-RNase monomer at this pH can be referred to the higher pI (10.3 versus 9.4) with respect to RNase A and to the fact that denaturation occurs at a lower temperature, so the exposure of MCM-BS-RNase at higher temperatures during each experiment happens for a limited time and for a restricted temperature range.

As it is reasonable to assume that the denatured states of the monomeric derivative of BS-RNase and of RNase A are energetically equivalent, the lower stability of the former must be due to less effective interactions in the monomeric derivative of BS-RNase. This finding is clearly consistent with the consideration that the higher ordered structure achieved in evolution by the BS-RNase polypeptide sequence is that of a dimer, whereas the monomeric state is that of a chemical derivative of the protein. Furthermore, our findings are in line with previous data in the literature. D'Ursi et al. (*44*) showed that the N-terminal peptide of MCM-BS-RNase is less tightly bound to the main body of the free monomer, with respect to RNase A and to the monomer linked to its partner in the dimeric structure. An important role in this respect appears to be played by Pro-19, a key residue (replacing Ala-19 of RNase A) in the linker peptide connecting the N-terminal α-helix to the protein main body. Computational (*45*) and thermodynamic (*39*) studies on an RNase A variant with Pro at position 19 have revealed the lower stability of such variant with respect to wild-type RNase A. Furthermore, a thermodynamic analysis has shown that the introduction of four residues in RNase A—the already cited Pro, Leu, and two Cys into positions 19, 28, 31, and 32, respectively (with the two Cys protected by carboxyamidomethyl groups)—confers to RNase A the same stability of the monomer of BS-RNase (*39*), the other 19 residue differences between the two proteins being unimportant.

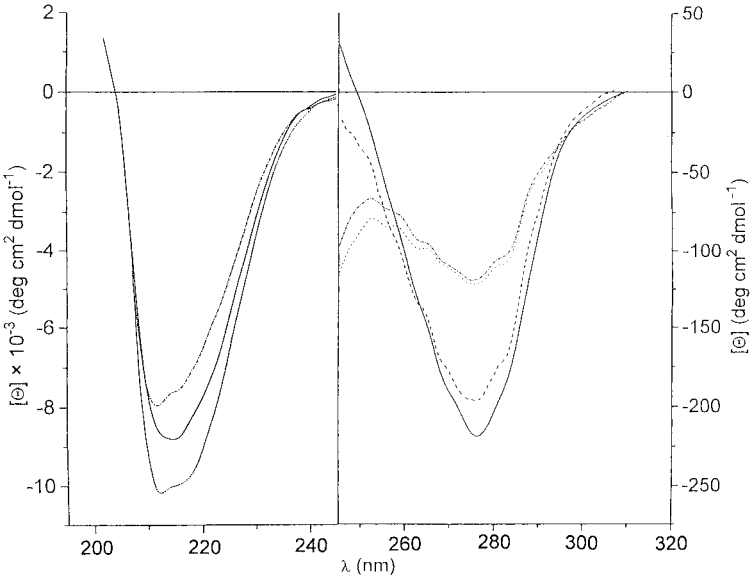

FIGURE 4: Far-UV CD spectra of M×M form (···), BS-RNase (−) and M═M form (-·-); and near-UV CD of RNase A (−), MCM-BS-RNase (- - -), M×M form (···) and M═M form (-·-), at pH 8.4 and 25 °C.

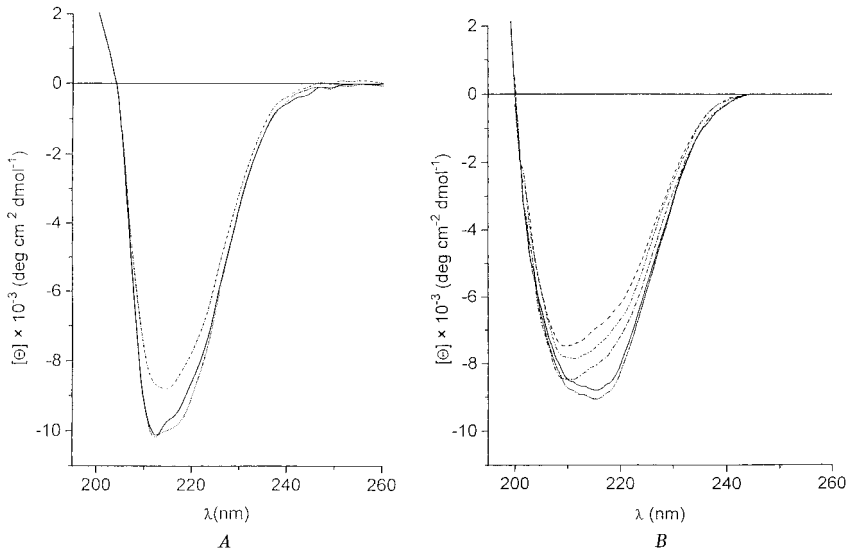

FIGURE 5: Far-UV circular dichroic spectrum of M×M form (···) (panel A), recorded after 7 h (−) and after 17 h (-·-); and of M═M form (- - -) (panel B), recorded after 1 day (-···-), after 2 days (-·-), after 5 days (−) and after 7 days (···), at pH 8.4 and 37 °C.

Circular Dichroism Analyses on the Isolated Isoforms of BS-RNase. In the CD spectra recorded in the far-UV region at 25 °C for the isolated isoforms of BS-RNase (Figure 4) a minimum around 212 nm and a shoulder around 216 nm are detected, with a higher intensity in the M×M spectrum, which suggests a greater content of secondary structure. More interesting is the finding that this fine structure is not detectable in the spectrum of BS-RNase. This shows, as previously found (*26*), a single smoothed minimum around 215 nm of intermediate intensity between those of the pure forms, but closer to that of M×M, as it would be expected for a mixture of one-third of M═M and two-thirds of M×M.

To investigate this question, the experiment illustrated in Figure 5 was performed. The isolated M×M form was incubated at 37 °C for prolonged time periods, under the conditions in which the M×M ⇔ M═M interconversion takes place (*5*). After 7 h, a change in the spectrum was observed, as this became more similar to that of BS-RNase equilibrium mixture. After a total of 17 h, the CD spectrum became undistinguishable from that of native BS-RNase at equilibrium. An analogous experiment was performed with the isolated M═M form. After a much longer incubation time, up to 7 days, the spectrum shown in Figure 5 was obtained, also in this case very similar to that of native BS-RNase at equilibrium. These findings suggest that in the equilibrium mixture of the two quaternary isoforms, i.e., in native BS-RNase, a loss of fine structure in the spectrum occurs. This loss is due to the superposition of the spectra of the isolated forms with those intermediate conformers. These intermediate conformers must be present at equilibrium, and indeed they have been detected in previous experiments (*36*).

The conclusion that the spectral features detected in the far UV region are due to local backbone conformational changes was confirmed by the finding that, in the spectra recorded in the near-ultraviolet regions (for sake of simplicity are reported only the case at pH 8.4 and 25 °C, Figure 4), no differences were found between the two forms. Further-

more, the spectra of both forms resemble that of the equilibrium mixture of native BS-RNase, as reported by Grandi et al. (*26*). In particular, these data indicate that the region comprising Tyr-73, the single tyrosine residue free to interact with the solvent in BS-RNase, is not involved in the M×M ⇔ M═M interconversion process. In fact, this region is far removed from the region involved in the displacement and exchange of the N-terminal α-helices between subunits.

CONCLUSIONS

BS-RNase quaternary structure, stabilized by the two disulfide bridges, is indispensable to attain a thermal stability comparable to that of its homologous RNase A and other mesophilic proteins, as shown by the results reported above. In fact, the isolated monomeric derivative is much less stable than the two dimeric isoforms. The denaturation processes of both the MxM and the M═M forms are three-state processes, but the monomeric subunits do not appear to play as intermediates in the process. Rather it is the central core of the dimers, stabilized by covalent bonds and hydrophobic interface, that melts in the second step of denaturation. This is an unusual behavior for the oligomeric proteins. The deconvolution of the DSC denaturation experiments outlines the apparent paradox that the more ordered M×M form starts to collapse at a lower temperature with respect to M═M (T_{d1} resulting about 2 °C lower for the M×M form at both pH 3.0 and 5.0). Since the $\Delta_{d1}H$s are equal, this effect may be imputable to a higher entropic gain for the M×M form than for the M═M form, in the transitions toward their respective intermediates. The second step in the three-state process, on the contrary, is enthalpy driven for both MxM and M═M (even if partially compensated by the entropy changes). This indicates a greater weakening of interactions and loss of order in the case of the structure characterized by the swapping of the N-terminal segments between subunits, assuming an identical behavior for the respective denatured states.

The results from the CD studies show that the isolated, more stable M×M form has a higher content of secondary structure than the M═M form, and both forms have a more evident fine structure than native BS-RNase. However, native BS-RNase is an equilibrium mixture in which all equilibrium intermediates between MxM and M═M are also present, most of them with a loss of secondary structure, due to the displacement and disordering of the N-terminal α-helices and of surrounding structural regions. Thus the CD data reveal the existence of intermediate conformers in the equilibrium mixture that we call BS-RNase.

REFERENCES

1. D'Alessio, G., Di Donato, A., Mazzarella, L., and Piccoli, R. (1997) in *Ribonucleases: Structures and Functions* (D'Alessio, G., and Riordan, J. F., Eds.) pp 383−423, Academic Press, New York.
2. Beintema, J. J., Breukelman, H. J., Carsana, A., and Furia, A. (1997) in *Ribonucleases: Structures and Functions* (D'Alessio, G., and Riordan, J. F., Eds.) pp 245−269, Academic Press, New York.
3. Mazzarella, L., Capasso, S., Demasi, D., Di Lorenzo, G., Mattia, C. A., and Zagari, A. (1993) *Acta Crystallogr., Sect. D 49*, 389−402.
4. Di Donato, A., Cafaro, V., Romeo, I., and D'Alessio, G. (1995) *Protein Sci. 4*, 1470−1477.
5. Piccoli, R., Tamburrini, M., Piccialli, G., Di Donato, A., Parente, A., and D'Alessio, G. (1992) *Proc. Natl. Acad. Sci. U.S.A. 89*, 1870−1874.
6. Youle, R. J., and D'Alessio, G. (1997) in *Ribonucleases: Structures and Functions* (D'Alessio, G., and Riordan, J. F., Eds.) pp 491−514, Academic Press, New York.
7. Vescia, S., Tramontano, D., Augusti-Tocco, G., and D'Alessio, G. *(*1980) *Cancer Res. 40*, 3740−3744.
8. Tamburrini, M., Scala, G., Verde, C., Ruocco, M. R., Parente, A., Venuta, S., and D'Alessio, G. (1990) *Eur. J. Biochem. 190*, 145−148.
9. Cafaro V., De Lorenzo, C., Piccoli, R., Bracale, A., Mastronicola, M. R., Di Donato, A., and D'Alessio, G. (1995) *FEBS Lett. 359*, 31−34.
10. Kim, J. S., Soucek, J., Matousek, J., and Raines, R. T. (1995) *J. Biol. Chem. 270*, 10525−10530.
11. D'Alessio, G., Malorni, M. G., and Parente, A. (1975) *Biochemistry 14*, 1116−1122.
12. Parente, A., Albanesi, D., Garzillo, A. M., and D'Alessio, G. (1997) *Ital. J. Biochem*.
13. Piccoli, R., and D'Alessio, G. (1984) *J. Biol. Chem. 259*, 693−695.
14. Barone, G., Del Vecchio, P., Fessas, D., Giancola, C., Graziano, G., Pucci, P., Ruoppolo, M., and Riccio, A. (1992) *J. Thermal Anal. 38*, 2791−2802.
15. Catanzano, F., Giancola, C., Graziano, G., and Barone, G. (1996) *Biochemistry 35*, 13378−13385.
16. Graziano, G., Catanzano, F., Giancola, C., and Barone, G. (1996) *Biochemistry 35*, 13386-13392.
17. Catanzano, F., Graziano G., Capasso, S., and Barone, G. (1997) *Protein Sci. 6*, 1682−1693.
18. Barone, G., Catanzano, F., Del Vecchio, P., Giancola, C., and Graziano, G. (1997) *Pure Appl. Chem. 69*, 2307−2313.
19. Tamburrini, M., Piccoli, R., De Prisco, R., Di Donato, A., and D'Alessio, G. (1986) *Ital. J. Biochem. 35*, 22−32.
20. D'Alessio, G., Floridi, A., De Prisco, R., Pignero, A., and Leone, E. (1972) Bull Seminal Ribonucleases 1. Purification And Physicochemical Properties Of The Major Component. *Eur. J. Biochem. 26*, 153−161.
21. D'Alessio, G., Floridi, A., De Prisco, R., Pignero, A., and Leone, E. (1972) *Eur. J. Biochem. 26*, 153−161.
22. Sela, M., Anfisen, C., and Harrington, W. (1957) *Biochim. Biophys. Acta 24*, 229−239.
23. Barone, G., Del Vecchio, P., Fessas, D., Giancola, C., and Graziano, G. (1992) *J. Thermal Anal. 38*, 2779−2790.
24. Freire, E., and Biltonen, R. L. (1978) *Biopolymers 17*, 463−479.
25. Privalov, P. L. (1979) *Adv. Protein Chem. 33*, 167−241.
26. Grandi, C., D'Alessio, G., and Fontana, A. (1979) *Biochemistry 18*, 3413−3420.
27. Puett, D. (1972) *Biochemistry 11*, 1980−1190.
28. Dill, K. A. (1990) *Biochemistry 29*, 7133−7155.
29. Filimonov, V. V., Potekhin, S. V., Matveyev, S. V., and Privalov, P. L. (1982) *Mol. Biol. (URSS) 16*, 551−562.
30. Privalov, P. L., and Potekhin, S. V. (1986) *Methods Enzymol. 131*, 4−51.
31. Marquardt, D. (1963) *J. Appl. Math. 11*, 431−441.
32. Catanzano, F., Gambuti, A., Graziano, G., and Barone, G. (1997) *J. Biochem. 121*, 568−577.
33. Battistel, E., Bianchi, D., and Rialdi, G. (1991) *Pure Appl. Chem. 63*, 1483−1490.
34. Labhardt, A. M. (1984) *Proc. Natl. Acad. Sci. U.S.A. 81*, 7674−7678.
35. De Lorenzo, C., Dal Piaz, F., Piccoli, R., Di Maro, A., Pucci, P., and D'Alessio, G. (1998) *Protein Sci. 7*, 2653−2658.
36. Piccoli, R., De Lorenzo C., Dal Piaz, F., Pucci, P., and D'Alessio, G. (2000) *J. Biol. Chem. 275*, 8000−8006.
37. Brandts, J., F., Hu, C., Q., and Lin, L. (1989) *Biochemistry 28*, 8588−8596
38. Sica, F., Adinolfi, S., Berisio, R., De Lorenzo, C., Mazzarella, L., Piccoli, R., Vitagliano, L., and Zagari, A. (1999) *J. Cryst. Growth 196*, 305−312.

39. Catanzano, F., Graziano, G., Cafaro, V., D'Alessio, G., Di Donato, A., and Barone, G. (1997) *Biochemistry 36*, 14403−14408.
40. Murphy, K. P., and Freire, E. (1992) *Adv. Protein Chem. 43*, 313−361.
41. Makhatadze, G. I., and Privalov P. L. (1995) *Adv. Protein Chem 47*, 307−425.
42. Barone, G., Del Vecchio, P., Giancola, C., and Graziano, G. (1995) *Int. J. Biol. Macromol. 17*, 251−257.
43. Graziano, G., Catanzano, F., Del Vecchio, P., Giancola, C., and Barone, G. (1996) *Gazz. Chim. It. 126*, 559−567.
44. D'Ursi, A., Oschkinat, H., Cieslar, C., Picone, D., D'Alessio, G., Amodeo, P., and Temussi P. A. (1995) *Eur. J. Biochem. 229*, 494−502.
45. Mazzarella, L., Vitagliano, L., and Zagari, A. (1995) *Proc. Natl. Acad. Sci. U.S.A. 92*, 3799−3803.

BI992953J